MAGNETIC RESONANCE IN CHEMISTRY
Magn. Reson. Chem. **36**, S161–S168 (1998)

Combined use of NMR and molecular modelling calculations for the conformational analysis of the TraM headpiece†

T. Stockner, C. Plugariu and H. Sterk*

Institut für Organische Chemie, Karl-Franzens-Universität Graz, Heinrichstrasse 28, 8010 Graz, Austria

Received 10 November 1997; revised 2 February 1998; accepted 2 February 1998

ABSTRACT: The *N*-terminal headpiece, MAKVQAYVSDEIVYKINKIVER, of the TraM protein exists in two distinct conformers in a water–SDS mixture. ^{1}H NMR investigations and X-PLOR calculations revealed that one of the conformers has a helical structure whereas in the other conformer the helical structure is bent at E-11. The two structures are characterized by different chemical shifts for the Hα and NH protons of S-9 and D-10. © 1998 John Wiley & Sons, Ltd.

KEYWORDS: NMR; ^{1}H NMR; TraM protein headpiece; structure analysis

INTRODUCTION

Based on mutational analyses, it was shown that the TraM protein, which is essential for the conjugative transfer of the F-like resistance plasmid R1,[1] has a dual role in this process. First, a functional TraM protein was found to be required for normal levels of transfer gene expression. The second function is probably a direct involvement of TraM in the structural and functional organization of the nucleoprotein complex at the origin of conjugative DNA transfer, *oriT*.[2,3]

Experiments with mutants suggest that the sequence specific DNA-binding and autoregulatory capacity of the TraM protein is conferred by the *N*-terminal 22 amino acids.[1,4] For mutants which produce the change of two amino acids, Val at position 20 with Glu and Glu at position 21 with Gly, the DNA-binding capacity of the protein has no longer been found. When the DNA-binding ability of the TraM protein was monitored indirectly by an *in vivo* autoregulation assay, mutations which produced changes of hydrophobic to polar amino acids in this region led to a considerable decrease in the DNA-binding capacity of the protein. Specifically, replacing a Val at position 20 with Glu, or Ile at position 12 with Arg, had more dramatic effect on autoregulation than even the loss of the 71 amino acid *C*-terminal part of TraM.[1,4] Since R1 plasmids producing mutant TraM proteins which are not functional in DNA binding or autoregulation are also deficient in conjugation,[1] the biological function of TraM can be related to the presence of a functional *N*-terminal structure.

In this work, a 22-amino acid peptide containing the *N*-terminal end of the TraM protein[5] was analysed by NMR in water–SDS solution to mimic a membrane environment. The structures were calculated with the X-PLOR molecular modelling package.

Experimental

The linear peptide MAKVQAYVSDEIVYKINKIVER was provided by Pi-Chem (Graz, Austria). The product was purified by preparative HPLC using a water–acetonitril gradient, and was checked for authenticity using MALDI-TOF mass spectrometry. Perdeuterated SDS (SDS-d_{25}, 98.6% D) was purchased from Isotec and D_2O (99.8% D) from Aldrich.

A 3 mg ml^{-1} solution of the peptide was prepared in H_2O containing 5% of D_2O, the pH being adjusted to 5. SDS-d_{25} was added to give a 30:1 molar ratio of SDS with respect to the TraM headpiece peptide. The spectra were recorded at 294 K using a Varian 600 MHz Inova Unity spectrometer. Water suppression was performed using the WATERGATE technique.[6]

Homonuclear shift correlations were determined from a TOCSY[7] experiment with a mixing time of 70 ms and a spectral width of 5687 Hz in both dimensions. The data set was composed of 4K FIDs compiled from 80 transients and 207 increments in t_1. Prior to Fourier transformation the data were apodized in both dimensions by shifted squared sine-bell functions.

Interatomic distances were established using phase sensitive NOESY spectra,[8] with mixing times of 200 and 300 ms and a spectral width of 5687 Hz in both dimensions. The NOESY experiment with a 200 ms mixing time was composed of 4K data points, 128 transients and 256 increments in t_1 and a 300 ms mixing

* *Correspondence to*: H. Sterk, Institut für Organische Chemie, Karl-Franzens-Universität Graz, Heinrichstrasse 28, 8010 Graz, Austria.
E-mail: heinz.sterk@kfunigraz.ac.at
† Dedicated to Professor John D. Roberts on the occasion of his 80th birthday.
Contract/grant sponsor: Fonds zur Förderung der wissenschaftlichen Forschung; *Contract/grant number*: 11048

CCC 0749-1581/98/SI0161–08 $17.50

time, 4K data points, 80 transients, and 238 increments in t_2. All spectra were analysed using the program ANSIG;[9,10] the chemical shifts are listed in Table 1.

The methyl and methylene groups were not stereospecifically assigned and were treated as pseudoatoms[11] using the centre average method.[12] The NOE distance constraints were divided into three groups: strong (1.8–2.7 Å), medium (1.8–3.6 Å) and weak (1.8–5.0 Å); for comparison, see Ref. 13.

The structure calculations from experimental distance constraints were performed using the program X-PLOR[12] on Silicon Graphics Power Challenge workstations. The calculations were set out from an extended strand[14] employing the protocols generate.inp, generate_template.inp, dg_sub_embed.inp, dg_full_embed.inp, dgsa.inp, and refine.inp.[14–16] The energies (Table 2) of the minimized structures were calculated with the modified CHARMM force field of X-PLOR.

Results and Discussion

Taking into account the sequence of the amino acids MAKVQAYVSDEIVYKINKIVER of the TraM head-

Table 1. Chemical shifts of the TraM headpiece

	Chemical shifts (ppm) of the TraM headpiece peptide[a]					
Residue	NH	Hα	Hβ	Hγ	Hδ	Other
Met-1		4.22	2.22, 2.29	2.62		
Ala-2	8.63	4.35	1.50			
Lys-3	8.13	4.29	1.92	1.50, 1.59	1.76	Hε 3.05
Val-4	7.77	3.93	2.23	1.00, 1.06		
Gln-5	8.19	4.03	2.08, 2.14	2.42, 2.44		
Ala-6	7.91	4.14	1.35			
Tyr-7	7.87	4.40	3.16, 3.05			H3,5 6.79; H2,6 7.12
Val-8	7.89	3.91	2.21			
Ser-9	8.06	4.34	3.94, 4.06			
Ser-9	8.03	4.36	3.94, 4.06			
Asp-10	8.42	4.54	2.89, 3.01			
Glu-11	8.16	4.33	2.01, 2.08	2.41, 2.45		
Ile-12	7.92	3.89	2.15	1.27, 1.72	0.95	
Val-13	7.87	3.57	2.11	0.91, 1.02		
Tyr-14	7.68	4.32	3.14			H3,5 6.85; H2,6 7.14
Lys-15	7.82	4.05				
Ile-16	8.20	3.78	2.00	1.17, 1.79	0.85	CH_3 γ 0.94
Asn-17	8.33	4.44	2.72, 2.85			
Lys-18	7.61	4.05	1.89	1.40, 1.49	1.65	Hε 2.94, 3.00
Ile-19	7.72	3.97	2.04	1.27, 1.73	0.89	CH_3 γ 0.96
Val-20	7.96	3.99	2.23	0.99, 1.03		
Glu-21	7.88	4.35	2.04, 2.19	2.51, 2.57		
Arg-22	7.81	4.27	1.91, 1.99	1.72	3.24	NH 7.17

[a] Chemical shifts are reported with respect to the water signal at 4.78 ppm.

Table 2. Calculation statistics for the TraM headpiece[a]

	R.m.s. differences (Å) ⟨SA⟩ vs SA_{av}	
Residue	Backbone r.m.s. differences	Non-hydrogen r.m.s. differences
1–8	0.50	4.08
12–22	0.47	8.66
Conformer	$E_{L\text{-}J}$ (kcal mol^{-1})	
I	332.73 ± 69.48	
II	383.15 ± 51.63	

[a] Notation is as follows: ⟨SA⟩ is the average value of the 31 simulated annealing structures; SA_{av} is the mean structure obtained by averaging the coordinates of the individual simulated annealing structures best fitted to each other; the structures are minimized with the X-PLOR force field. $E_{L\text{-}J}$ is the average energy calculated with the modified CHARMM force field of X-PLOR.

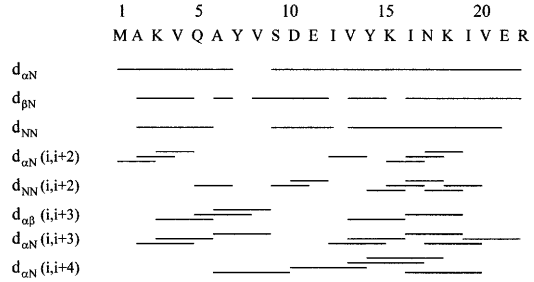

Figure 1. Illustration of the short- and medium-range NOEs involving NH, Hα and Hβ protons of the TraM headpiece.

piece, it is immediately obvious that there is a more or less regular arrangement of alternating polar and non-polar amino acids. Our NMR investigations of the TraM headpiece in a water–SDS mixture yielded a set

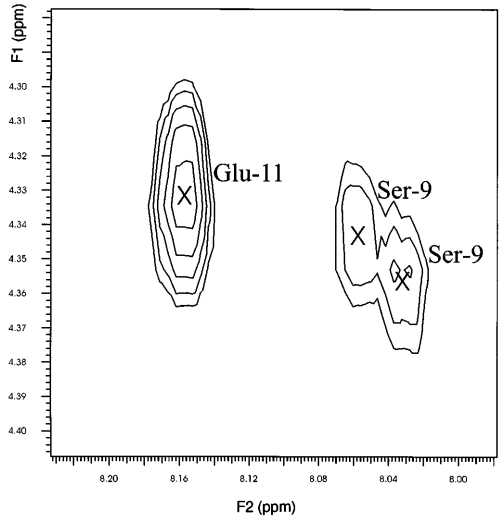

Figure 2. Region of the TOCSY spectrum around the Ser-9 NH–Hα cross peak showing two chemical shifts for the NH and Hα protons.

of 60 short-range and 87 medium-range NOE cross peaks between the NH, Hα and Hβ and also the aromatic protons (Fig. 1). These data allow us to construct a network of interatomic distances, which reflect the structure of the peptide in solution. It should be noted, however, that there are some problems in generating a complete peptide structure from the present NOE data.

There are no problems for the *C*-terminal domain from Ile-12 to Arg-22, since all relevant medium distant cross peaks are well resolved and the complete NOE pattern exhibits all characteristics of a helical structure. On account of two unfortunate circumstances, no such clear conclusion can be drawn about the 2D structure of the *N*-terminal part. On the one hand, the severe spectral overlap of several important cross peaks defeats an unambiguous assignment of certain interatomic distances. On the other hand, the actual cross peak pattern lacks some NOE signals of medium-distant proton–proton interactions, which are mandatory for a perfect helical structure. Moreover, the assignment procedure for this *N*-terminal TraM part revealed the surprising result that Ser-9 gives rise to two series of signals of equivalent intensities. The chemical shift differences between these corresponding signals are especially large for the NH and Hα peaks (NH 0.025 ppm; Hα 0.020 ppm), as can be seen in Fig. 2. A similar signal doubling, but with considerably smaller shift differences, could be detected for Asp-10. These observations can be rationalized only by assuming that the TraM headpiece exists in two distinct conformers on the NMR time-scale, which differ significantly in the region around Ser-9 and Asp-10.

Based on our present knowledge, a discrimination between a slow exchange on the NMR time-scale between micellar-bound and free molecules or two distinct conformers cannot be drawn. However, it is obvious that this phenomenon is not caused by

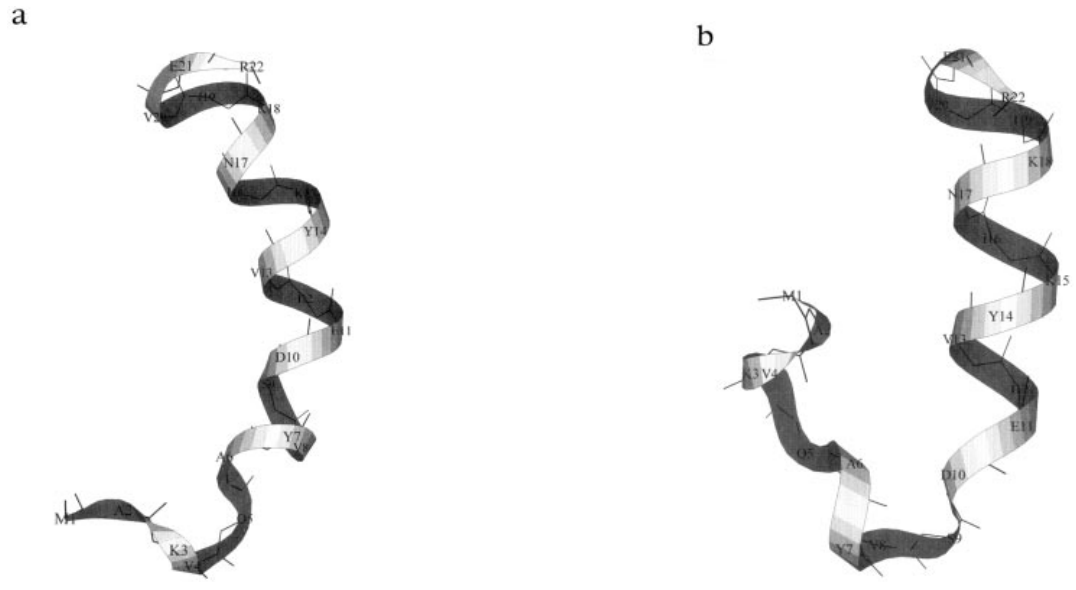

Figure 3. Schematic representation of a calculated structure. (a) Conformer I and (b) conformer II.

racemization as the peptide solution in water behaves in the proper way.

For further elucidation of the *N*-terminal TraM structure in general and this conformational duality in particular, we performed modelling calculations with the program X-PLOR. All cross peaks, as shown in Fig. 1, were employed as constraints in the structure-generating procedure. Nine out of a total initial set of 40 generated structures were not in full compliance with all constraints and, consequently, were not taken into further consideration. The remaining 31 structures, which are in complete conformity with all prescribed NOE constraints, exhibit a common structural feature, i.e. an α-helix from Ile-12 to Val-20. This helical pattern is unambiguously corroborated by a large set of medium-range NOE cross peaks (r.m.s. differences 0.50 Å).

The amino acid sequence within the helical region leads to a strict steric ordering in that all hydrophobic and all polar residues lie on opposite sides of the helix, as can be seen in Figs 3(a) and 4(a). The invariability of such an amphiphilic helix in all optimized structures allows one to infer that this helical segment is common to both TraM headpiece conformers in question, and in agreement with the corresponding cross peak data. The structural dissimilarities are confined to the *N*-terminal part.

The modelling calculations predict two conformers [Fig. 4(b)]. These two conformers differ in this part of the 2D structure which contains Glu-11, Asp-10 and Ser-9. Thereby the conformer (**I**) with the lower energy (332.7 kcal mol^{-1}) shows the α-helix from Ile-12 extending down to Ala-6 [Fig. 3(a)]. The second conformer (**II**) with an energy of about 383.1 kcal mol^{-1} can be char-

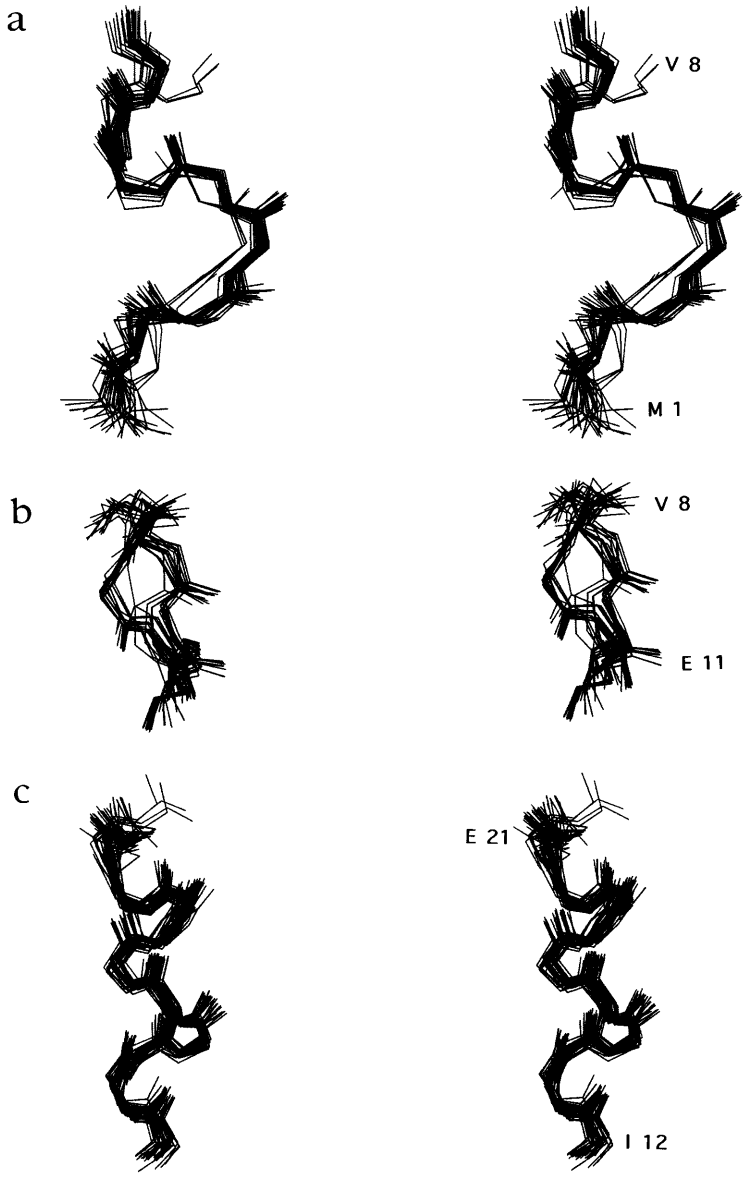

Figure 4. Stereoviews of the superposition of the 31 calculated structures which fulfil all NOE restraints. (a) Superposition of all 31 structures from residue Ile-12 to Arg-22, showing the well defined α-helix from Ile-12 to Val-20. (b) Superposition of all 31 structures from residue Val-8 to Glu-11, showing the two conformers. (c) Superposition of the first eight residues.

Table 3. Scalar coupling constants and average ϕ and ψ Ramachandran angles[a]

		Conformer **I**		Conformer **II**	
Amino acid	J (NH, HA) (Hz)	ϕ	ψ	ϕ	ψ
2	5.4	88.9	56.1	88.9	56.1
3	6.6	−106.3	24.7	−106.3	24.7
4	4.8	−78.5	−32.0	−78.5	−32.0
5	4.8	144.5	25.0	144.5	25.0
6	5.4	−33.1	−47.9	−33.1	−47.9
7	6.6	−24.5	−32.7	−24.5	−32.7
8	6.0	−35.5	−31.7	−35.5	−31.7
9a	4.2	−122.7	−19.4	−122.7	−19.4
9b	6.6	−122.7	−19.4	−122.7	−19.4
10	4.2	−19.3	−25.5	56.1	87.6
11	6.6	−79.2	−59.7	168.9	−59.7
12	6.0	−47.3	−46.5	−47.3	−46.5
13	—	−52.2	−43.4	−52.5	−43.4
14	4.2	−45.9	−41.8	−45.9	−41.8
15	7.2	−75.4	−15.3	−75.4	−15.3
16	6.6	−82.1	−56.7	−82.1	−56.7
17	—	−41.1	−35.0	−41.1	−35.0
18	3.6	−61.7	−23.4	−61.7	−23.4
19	3.6	−102.9	−53.0	−102.9	−53.0
20	5.4	−37.8	−35.6	−37.8	−35.6
21	6.0	138.9	28.9	138.9	28.9
22	4.8				

[a] The listed Ramachandran angles are the average angles obtained from 31 calculated structures (see also Tables 4 and 5). The scalar couplings between the NH and the Hα protons which are not listed could not be unravelled owing to severe overlap.

acterized by the fact that at position Glu-11 the α-helix is interrupted and the backbone is bent down at Asp-10 [Fig. 3(b)]. The rest of the *N*-terminal part, similarly to the first conformer, is helically arranged.

Looking at the 31 calculated structures, it turned out that 20 of them reflect the backbone situation of the helical conformer (**I**) whereas the rest of the calculated structures show the backbone type of the bend conformer (**II**). Within each conformer type, the different structures and energies are caused by various side-chain arrangements. As there are some cross peaks missing or overlapped which are relevant for medium-sized distance constraints in perfect α-helices, it is not unexpected that the calculated structures exhibit enhanced flexibilities. Especially the ϕ and φ angles of Ser-9 show high flexibility. It is not surprising, therefore, that X-PLOR calculations lead to three structures which reveal for the *N*-terminal part of both conformers poorly ordered structures. It is worth noting, however, that the energies of these poorly ordered structures are a good deal (*ca.* 150 kcal mol^{-1}) above the α-helix structure. All calculated structures are shown in Fig. 4(a)–4(c). Figure 4(c) represents a sketch of this *N*-terminal domain for all 31 modelled structures.

Conclusion

For a water–SDS mixture it has been shown that the headpiece of the TraM protein exists in two distinct conformers on the NMR time-scale which are energetically comparable. Both conformers form a regular α-helical part from Ile-12 to Val-20. In one conformer this helix is further extended down to Ala-6, whereas in the second conformer the helix is bent at Glu-11.

Acknowledgement

Generous contributions from the Fonds zur Förderung der wissenschaftlichen Forschung, Project 11048, are gratefully acknowledged.

Table 4. Ramachandran ϕ angles

Structure	Ala-2	Lys-3	Val-4	Gln-5	Ala-6	Tyr-7	Val-8	Ser-9	Asp-10	Glu-11	Ile-12	Val-13	Tyr-14	Lys-15	Ile-16	Asn-17	Lys-18	Ile-19	Val-20	Glu-21
1	45.9	−102.4	−74.0	−85.2	45.1	64.9	56.2	−85.5	−39.8	−55.3	−53.5	−60.6	−49.6	−88.7	−157.0	−43.4	−58.3	−90.5	−36.7	173.1
2	166.1	−102.8	−77.7	167.0	−40.7	−41.0	−42.5	−133.4	−41.0	−85.2	−42.3	−45.8	−42.7	−75.5	−77.5	−41.2	−59.1	−102.4	−36.9	173.5
3	46.8	−119.7	−80.6	171.5	−40.7	−40.9	−42.5	−133.3	−41.0	−85.3	−42.3	−45.8	−42.8	−73.0	−77.1	−40.6	−68.5	−98.8	−38.5	171.1
4	65.6	−102.7	−77.7	167.1	−40.7	−41.0	−42.6	−88.7	66.0	−84.6	−41.5	−44.2	−42.4	−72.4	−77.0	−40.6	−68.6	−98.4	−38.6	171.2
5	166.1	−102.9	−77.7	167.1	−40.7	−41.0	−42.7	−98.7	−40.7	−86.8	−44.9	−47.2	−42.4	−75.4	−77.5	−41.2	−59.1	−102.8	−37.0	173.5
6	65.4	−112.5	−81.6	172.2	−40.6	−41.0	−42.4	−112.9	−41.5	−85.6	−47.4	−43.4	−41.8	−71.6	−77.2	−40.8	−67.6	−101.1	−42.4	−89.8
7	166.1	−102.5	−77.6	167.1	−40.7	−41.0	−42.6	−174.1	67.0	171.1	−51.3	−54.1	−45.0	−76.5	−94.9	−41.4	−60.4	−126.8	−35.0	172.2
8	166.1	−102.8	−77.5	167.1	−42.1	−51.9	−105.1	−111.7	66.0	−84.5	−41.5	−44.1	−42.2	−75.4	−77.5	−41.2	−59.1	−102.5	−37.0	173.5
9	166.1	−120.8	−80.8	171.5	−40.7	−40.9	−42.6	−115.5	48.0	168.0	−51.4	−54.7	−45.5	−76.6	−103.5	−40.4	−62.0	−105.3	−37.3	173.5
10	43.0	−102.3	−74.0	−85.3	45.2	64.2	55.8	−85.6	67.3	170.9	−49.1	−59.5	−50.1	−75.3	−77.8	−41.0	−59.1	−103.1	−37.0	173.1
11	65.8	−127.8	−82.7	173.3	−40.4	−41.0	−42.6	−173.4	−39.9	−55.0	−53.3	−61.7	−50.9	−74.7	−77.8	−41.1	−59.3	−107.0	−36.9	173.4
12	166.1	−110.6	−79.3	171.5	−40.7	−40.9	−42.5	−124.2	49.8	167.6	−48.9	−58.4	−49.4	−74.3	−77.6	−40.6	−68.0	−99.8	−38.6	171.4
13	65.7	−108.6	−81.4	172.2	−40.6	−41.0	−42.5	−174.1	66.6	173.0	−47.3	−58.0	−49.0	−75.5	−77.8	−41.1	−59.1	−103.0	−37.0	173.5
14	166.1	−109.7	−79.3	171.5	−40.6	−40.8	−42.6	−125.0	−40.0	−55.0	−53.2	−61.7	−50.9	−75.1	−77.9	−41.0	−59.2	−102.9	−37.1	173.5
15	166.1	−94.6	−80.3	171.5	−40.7	−40.9	−42.5	−93.5	−41.5	−85.8	−47.8	−44.0	−41.8	−73.1	−77.4	−41.2	−59.3	−107.1	−37.0	173.5
16	46.9	−102.7	−77.8	167.1	−40.7	−41.0	−42.6	−174.3	66.8	167.8	−49.0	−59.7	−50.7	−74.8	−77.7	−41.0	−59.4	−106.9	−37.0	173.4
17	43.0	−102.9	−77.8	167.1	−40.8	−41.1	−42.6	−124.4	51.2	167.6	−48.9	−58.4	−49.3	−73.4	−77.4	−40.7	−69.0	−98.1	−38.6	171.3
18	65.5	−107.6	−80.4	171.4	−40.7	−40.9	−42.6	−120.3	50.2	167.6	−48.8	−58.4	−49.4	−75.3	−77.8	−41.0	−59.2	−103.1	−37.0	173.5
19	63.2	−102.7	−77.7	167.0	−40.8	−41.0	−42.5	−155.6	68.5	−58.9	−49.9	−58.1	−50.4	−74.9	−77.8	−41.1	−59.2	−103.2	−37.1	173.4
20	47.4	−102.7	−77.7	167.1	−40.7	−41.0	−42.5	−119.0	49.4	167.5	−49.0	−58.4	−49.4	−75.3	−77.8	−41.1	−59.2	−103.1	−37.1	173.5
21	43.0	−102.7	−77.7	167.0	−40.8	−41.0	−42.6	−124.2	50.3	167.6	−48.9	−58.4	−49.3	−75.5	−77.9	−41.1	−59.2	−102.8	−37.0	173.5
22	166.1	−102.6	−77.7	167.0	−40.8	−41.0	−42.7	−99.4	−40.9	−75.1	−54.8	−52.9	−47.6	−72.5	−77.8	−41.1	−59.1	−103.0	−37.1	173.5
23	51.2	−103.0	−77.7	167.1	−40.7	−41.0	−42.6	−133.4	−40.9	−85.3	−42.2	−45.9	−42.8	−72.2	−76.9	−40.6	−69.1	−98.1	−38.6	171.2
24	43.1	−102.5	−77.8	167.1	−40.7	−41.0	−42.5	−126.3	−40.5	−86.7	−43.9	−48.9	−42.9	−75.5	−77.4	−41.1	−59.1	−102.7	−37.0	173.5
25	42.9	−102.8	−77.7	167.1	−40.7	−41.1	−42.5	−125.6	−40.5	−86.6	−43.9	−48.9	−42.9	−75.4	−77.5	−41.1	−59.1	−102.8	−37.1	173.5
26	57.5	−120.2	−80.7	171.5	−40.6	−40.9	−42.6	−134.5	−40.5	−86.6	−43.9	−48.9	−42.9	−76.3	−77.6	−41.1	−58.9	−94.0	−42.2	−91.8
27	46.6	−102.6	−77.7	167.0	−40.8	−41.0	−42.6	−82.1	65.9	−84.6	−41.7	−43.8	−42.2	−87.8	−76.1	−42.2	−60.6	−125.7	−35.1	171.6
28	43.2	−102.4	−74.0	−85.2	45.2	64.8	56.2	−85.5	−41.2	−85.8	−47.8	−44.2	−41.9	−73.6	−77.6	−41.0	−59.0	−93.9	−42.2	−91.8
29	44.0	−102.7	−77.7	167.1	−40.7	−41.0	−42.6	−124.2	50.1	169.5	−48.1	−58.1	−49.1	−75.5	−77.8	−41.1	−59.1	−102.9	−37.1	173.5
30	166.1	−94.6	−80.1	171.5	−62.2	164.6	−57.1	−95.8	−41.1	−86.2	−46.7	−45.2	−41.7	−70.4	−96.3	−40.6	−77.3	−96.4	−42.3	−89.5
31	58.9	−118.8	−80.7	171.5	−40.7	−40.9	−42.5	−148.6	−40.8	−85.1	−42.1	−46.0	−42.8	−75.6	−77.5	−41.2	−59.1	−102.6	−37.0	173.5
Averaged angles	88.9	−106.3	−78.5	144.5	−33.1	−24.5	−35.5	−122.7			−47.3	−52.2	−45.9	−75.4	−82.1	−41.1	−61.7	−102.9	−37.8	138.9
Averaged angle, conformer **I**									−19.7	−79.2										
Averaged angle, conformer **II**									56.1	168.9										

Table 5. Ramachandran ψ angles

Structure	Ala-2	Lys-3	Val-4	Gln-5	Ala-6	Tyr-7	Val-8	Ser-9	Asp-10	Glu-11	Ile-12	Val-13	Tyr-14	Lys-15	Ile-16	Asn-17	Lys-18	Ile-19	Val-20	Glu-21
1	55.1	23.2	−31.5	−67.1	39.0	8.2	10.0	−43.0	−31.8	−34.8	−44.6	−43.0	−38.4	51.1	−57.2	−49.1	−17.6	−58.4	−33.2	29.8
2	55.1	24.6	−31.7	35.1	−61.5	−38.2	−37.1	13.0	−37.9	−64.6	−49.0	−43.7	−45.4	−16.9	−58.7	−35.6	−20.4	−59.0	−33.3	29.6
3	56.0	25.1	−32.4	34.0	−61.4	−38.0	−37.4	13.2	−38.0	−64.6	−49.0	−43.7	−45.6	−18.2	−58.5	−33.8	−38.2	−33.6	−38.3	29.5
4	55.7	24.7	−31.7	35.2	−61.5	−38.2	−37.1	−45.6	8.5	−63.5	−49.6	−43.7	−46.9	−18.5	−58.4	−33.6	−38.3	−33.6	−38.4	29.7
5	55.1	24.8	−31.7	35.1	−61.5	−38.2	−37.1	−11.2	−33.6	−65.5	−43.9	−43.7	−46.0	−17.0	−58.7	−35.5	−20.4	−59.0	−33.2	29.6
6	56.1	25.2	−32.4	33.8	−61.3	−38.0	−37.3	−67.3	−30.2	−64.8	−44.8	−43.6	−49.6	−17.8	−58.5	−34.0	−31.8	−40.7	−44.0	23.5
7	55.2	24.7	−31.7	35.1	−61.6	−38.2	−37.1	−32.8	79.2	−63.0	−48.6	−44.0	−37.9	−25.9	−36.7	−34.3	−13.5	−51.5	−35.8	30.1
8	55.1	24.6	−31.6	32.8	−70.9	−18.3	−2.2	−49.9	8.5	−63.5	−49.7	−43.7	−46.5	−16.9	−58.7	−35.7	−20.4	−58.9	−33.2	29.7
9	55.5	25.1	−32.3	33.9	−61.5	−37.9	−37.3	−7.4	93.5	−61.6	−48.6	−44.0	−37.8	−19.7	−43.1	−29.4	−17.6	−59.2	−33.0	29.7
10	55.1	23.2	−31.5	−67.1	39.2	8.7	10.1	−40.8	64.9	−62.8	−47.7	−44.2	−36.3	−15.9	−58.9	−35.0	−20.4	−59.0	−33.2	29.6
11	58.4	25.2	−32.4	33.6	−61.3	−38.0	−37.5	48.0	−31.9	−34.3	−44.5	−43.1	−36.2	−16.0	−58.8	−34.4	−18.5	−59.0	−33.2	29.7
12	55.5	25.1	−33.1	33.9	−61.4	−38.0	−37.4	−11.0	94.6	−61.3	−47.9	−44.0	−37.1	−16.8	−58.7	−34.4	−37.8	−33.6	−38.6	29.6
13	63.3	25.1	−32.4	33.8	−61.3	−37.9	−37.4	−33.0	78.5	−63.6	−47.7	−44.1	−37.3	−15.8	−58.8	−35.1	−20.4	−59.0	−33.3	29.7
14	55.6	25.1	−33.1	33.9	−61.5	−38.1	−37.3	−9.2	−31.9	−34.3	−44.5	−43.1	−36.2	−15.7	−58.9	−35.1	−20.4	−59.0	−33.2	29.6
15	58.1	25.2	−32.4	33.9	−61.4	−38.1	−37.4	−49.4	−28.9	−64.6	−43.9	−43.6	−49.1	−17.2	−58.7	−34.8	−18.1	−58.9	−33.3	29.7
16	55.7	24.7	−31.7	35.1	−61.5	−38.2	−37.1	−32.8	78.9	−61.3	−47.5	−44.2	−36.0	−16.1	−58.8	−34.4	−18.4	−59.0	−33.2	29.7
17	55.7	24.7	−31.7	35.1	−61.5	−38.1	−37.1	−10.5	95.3	−61.3	−47.8	−44.1	−37.1	−17.4	−58.6	−33.0	−38.3	−33.7	−38.4	29.6
18	56.3	25.2	−32.4	33.9	−61.4	−37.9	−37.4	−9.0	94.7	−61.3	−47.9	−44.1	−37.0	−15.9	−58.8	−34.9	−20.3	−59.0	−33.2	29.6
19	55.7	24.6	−31.6	35.1	−61.5	−38.2	−37.1	−82.0	5.2	−39.3	−50.4	−42.5	−36.9	−15.9	−58.8	−34.8	−20.3	−59.1	−33.2	29.7
20	55.7	24.7	−31.7	35.1	−61.5	−38.2	−37.1	−8.8	94.3	−61.2	−47.8	−44.0	−37.1	−15.9	−58.8	−35.0	−20.3	−59.0	−33.2	29.7
21	55.7	24.6	−31.7	35.1	−61.6	−38.2	−37.1	−10.9	94.7	−61.3	−47.7	−44.1	−37.1	−15.8	−58.8	−35.1	−20.4	−59.0	−33.2	39.6
22	55.1	24.7	−31.7	35.2	−61.5	−38.2	−37.0	−22.7	−27.8	−58.5	−33.7	−34.6	−44.6	−15.8	−58.9	−35.1	−20.4	−59.0	−33.2	29.6
23	55.7	24.7	−31.7	35.2	−61.6	−38.1	−37.1	13.0	−38.0	−64.6	−49.0	−43.7	−45.7	−18.5	−58.5	−33.1	−38.2	−33.7	−38.5	29.7
24	55.7	24.8	−31.7	35.1	−61.5	−38.2	−37.1	0.6	−37.0	−65.2	−44.0	−43.8	−44.7	−16.9	−58.7	−35.5	−20.4	−59.0	−33.3	29.7
25	55.8	24.7	−31.7	35.1	−61.5	−38.1	−37.1	0.9	−37.1	−65.2	−44.1	−43.8	−44.8	−16.8	−58.7	−35.5	−20.4	−58.9	−33.2	29.6
26	56.0	25.2	−32.3	33.8	−61.4	−38.0	−37.4	3.1	−37.1	−65.2	−44.1	−43.8	−44.6	−16.4	−58.8	−36.5	−23.4	−59.7	−44.2	23.0
27	55.8	24.7	−31.7	35.2	−61.5	−38.2	−37.1	−48.6	8.5	−63.6	−49.6	−43.8	−47.9	−21.7	−58.0	−37.4	−13.2	−50.7	−35.8	30.6
28	55.1	23.2	−31.5	−67.1	39.0	8.3	9.9	−42.9	−29.3	−64.5	−43.9	−43.6	−49.0	−16.5	−58.8	−36.2	−23.6	−59.6	−44.2	23.0
29	55.7	24.7	−31.7	35.1	−61.6	−38.1	−37.1	−10.9	94.7	−62.2	−47.8	−44.0	−37.3	−15.8	−58.9	−35.1	−20.4	−59.0	−33.2	29.8
30	57.5	25.2	−32.3	45.4	68.1	−30.2	−42.4	−28.2	−30.6	−64.9	−43.9	−43.6	−44.6	−24.3	−34.7	−28.0	−32.2	−33.9	−43.9	23.5
31	56.0	25.2	−32.3	33.8	−61.4	−38.1	−37.4	15.5	−39.0	−64.4	−49.3	−43.7	−45.1	−16.9	−58.7	−35.5	−20.4	−58.9	−33.2	29.7
Average angles	56.1	24.7	−32.0	25.0	−47.9	−32.7	−31.7	−19.4		−59.7	−46.5	−43.4	−41.8	−15.3	−56.7	−35.0	−23.4	−53.0	−35.6	28.9
Averaged angle, conformer **I**									−25.5											
Averaged angle, conformer **II**									87.6											

REFERENCES

1. E. Pölzleitner, E. L. Zechner, W. Renner, R. Fratte, B. Jauk, G. Högenauer and G. Koraimann, *Mol. Microbiol.* **25**, 495 (1997).
2. G. Kupelweiser, G. Högenauer, G. Koraimann and E. L. Zechner, *J. Mol. Biol.* submitted for publication.
3. M. Schwab, H. Gruber and G. Högenauer, *Mol. Microbiol.* **5**, 439 (1991).
4. M. Schwab, H. Reisenzein and G. Högenauer, *Mol. Microbiol.* **7**, 795 (1993).
5. C. Plugariu, T. Stockner, D. Moskau, G. Koraimann and H. Sterk, *J. Pept. Res.* in press.
6. V. Sklenar, M. Piotto, R. Leppik and V. Saudek, *J. Magn. Reson. A* **102**, 241 (1993).
7. (a) A. Bax and D. G. Davis, *J. Magn. Reson.* **65**, 355 (1985); (b) L. Braunschweiler and R. R. Ernst, *J. Magn. Reson.* **53**, 521 (1983).
8. (a) A. Bax and D. G. Davis, *J. Magn. Reson.* **63**, 207 (1985); (b) A. A. Bothner-By, R. L. Stephens, J. Lee, C. D. Warren and R. W. Jeanloz, *J. Am. Chem. Soc.* **106**, 811 (1984).
9. P. J. Kraulis, *J. Magn. Reson.* **24**, 627 (1989).
10. P. J. Kraulis, P. J. Domaille, S. L. Campbell-Burk, T. van Aken and E. D. Laue, *Biochemistry* **33**, 3515 (1994).
11. K. Wüthrich, M. Billeter and W. Braun, *J. Mol. Biol.* **169,** 949 (1983).
12. A. T. Brünger, *X-PLOR* (*Version 3.1*). *A System for X-Ray Crystallography and NMR*. (1992).
13 K. Wüthrich, *NMR of Proteins and Nucleic Acids*. Wiley, New York (1986).
14. M. Nilges, G. M. Clore and A. M. Gronenborn, *FEBS Lett.* **229**, 317 (1988).
15. M. Nilges, J. Kuszewski and A. T. Brünger, *in Computational Aspects of the Study of Biological Macromolecules by NMR*, edited by J. C. Hoch. pp. 451–455. Plenum Press, New York (1991).
16. J. Kuszewski, M. Nilges and A. T. Brünger, *J. Biomol. NMR* **2**, 33 (1992).

